

Observations of HDO in the high-mass formation regions.

Magda Kulczak-Jastrzębska¹, Dariusz Lis^{2,3} and Maryvonne Gerin²

1. Astronomical Observatory of the Jagiellonian University, Orla 171, 30-244 Kraków, Poland; kulczak@oa.uj.edu.pl
2. École Normale Supérieure, CNRS, Observatoire de Paris, UMR 8112, LERMA, Paris, France
3. Caltech, Cahill Center for Astronomy and Astrophysics, 301-17, Pasadena, CA 91125, USA

Deuterated species are powerful tools to study the physical structure and dynamics of protostellar envelopes, yet their observations are still scarce. We present observations of the ground state $1_{0,1}-0_{0,0}$ rotational transition of HDO at 464.925 GHz and the $1_{1,0}-1_{0,1}$ transition at 509.292 towards three high-mass star forming regions, carried out with the Caltech Submillimeter Observatory. The latter transition is observed for the first time from the ground. The HDO lines are modeled using a spherically symmetric radiative transfer code to derive the radial distribution of the HDO abundance in the target sources. The abundance profile is divided into an inner hot core region, with $T > 100$ K and a cold outer envelope with $T < 100$ K. The H_2^{18}O observations from Flagey et al. (2013) are used to calculate the H_2O abundance profile and thus, allow us to constrain the HDO/ H_2O ratio in the envelopes of high-mass star forming regions.

1 Introduction

During the cold phase preceding the formation of stellar objects, molecules freeze-out onto dust grains, forming H_2O dominated ice mantles, dirtied with other less-abundant species. The low temperature and the disappearance of most molecules, especially CO from the gas phase trigger a peculiar chemistry leading to high abundances of deuterated species. Molecules tend to attach a D atom rather than an H atom, because deuterated species have larger reduced masses and consequently lower binding energies, arising from lower zero-point vibrational energies. Ion-molecule reactions in the gas phase (Brown & Millar, 1989) and reactions on the grain surfaces (Tielens, 1983) are the two possible mechanisms responsible for deuterium enrichments in heavy molecules. The reactions involved are exothermic and this is why significant deuteration levels can be expected in the cold ISM. In the warmer phase, only very little fractionation is expected to occur, because the energy barrier could be overcome by the elevated temperature. However, at the temperatures deduced for hot core regions (100 - 200 K) ice mantles evaporate and the gas again becomes enriched in deuterated species, with abundances elevated compared to the cosmic D/H ratio for a short period, before the chemistry reaches steady-state. These enhancements in hot cores reflect, to some degree, the grain mantle composition in earlier, colder cloud phases.

2 Determination of the HDO abundance

The goal of this study is to determine the HDO fractional abundance in the three high-mass stars formation regions: W49N, W51e1/e2, G34.26+0.15 (Table 1). To reproduce the observed line intensities (Table 2) the static radiative transfer code of Zmuidzinas et al. (1995) is used. We carried out model calculations from inner core radius, r_{min} , to outer radius, r_{max} (with $r_{min}/r_{max} \sim 100$ for all sources; Hatchell & van der Tak 2003). The distance of the edge of the core from the star is set at $r_{min} \sim 2.0 \times 10^{16}$ cm or ~ 1000 AU, with no dust emission seen at the smaller radii. We adopted a dust-to-gas ratio of 1:100 and a power-law H_2 density distribution of the form:

$$n(r) = n_0 \left(\frac{r}{r_{min}} \right)^{-1.5}, \quad (1)$$

where n_0 is the H_2 density at the reference radius ($r_{min} = 1000$ AU). The power-law index was set to 1.5 according to the static infall theory in the inner part of the object (Shu, 1977; Beuther et al., 2002; Marseille et al., 2010). We assumed that the gas and dust radial temperature profiles follow a power law (Viti & Williams, 1999):

$$T(r) = T_0 \left(\frac{r}{r_{min}} \right)^{-0.5}, \quad (2)$$

where T_0 represents the maximum temperature of dust grains. We assumed that at densities found in hot cores the gas temperature is equal to the dust temperature.

3 Observations

Observations of the 464 GHz and 509 GHz HDO transitions presented here were carried out in 2012 June–August, using the 10.4 m Leighton Telescope of the Caltech Submillimeter Observatory (CSO) on Mauna Kea, Hawaii. The CSO main-beam efficiency at 464 GHz at the time of the observations was determined from total-power observations of planets to be $\sim 37\%$. The absolute calibration uncertainty of the individual measurements is $\sim 20\%$. The data processing was done using the IRAM GILDAS software package (Pety, 2005).

4 Exemplary source G34.26+0.15

G34.26+0.15 is one of the best studied high-mass star forming regions in the Galaxy. Embedded within this molecular cloud is a hot core, which exhibits strong H_2O maser emission and high abundances of saturated molecules (MacDonald et al., 1996), two unresolved UC H II regions, labeled A and B, a more evolved H II region with a cometary shape, and an extended ring-like H II region (Reid & Ho, 1985). Based on narrow-band mid-infrared imaging of the complex Campbell et al. (2000) concluded that the same star is responsible for ionization of the cometary H II component (C) and heating the dust, but is not interacting with the hot core seen in the molecular emission. At a $12''$ resolution, Hunter et al. (1998) also found the peak of the $350 \mu\text{m}$ emission to coincide with the component C of the UC H II region.

Observed and best-fit model spectra of the 465 GHz and 509 GHz HDO transitions towards G34.26+0.15 are shown in Figure 1 (blue and red lines). Model results are presented in Table 2.

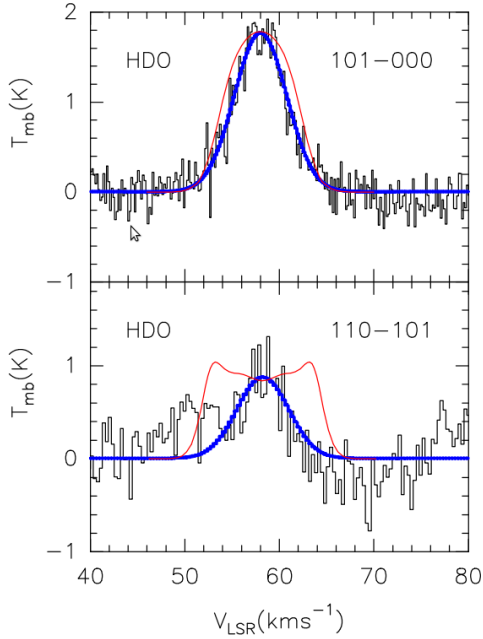


Fig. 1: Observed and best-fit model spectra of the 465 GHz and 509 GHz HDO transitions towards G34.26+0.15. Gaussian fits are shown in blue, together with the best-fit model in red.

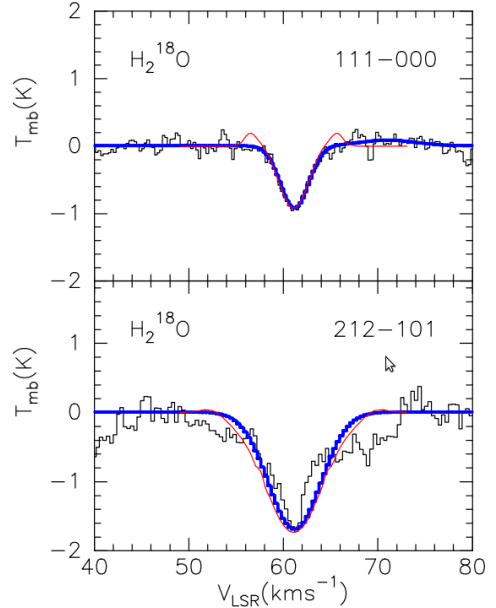


Fig. 2: Observed and modeled spectra of the para- H_2^{18}O line at 1102 GHz and the ortho- H_2^{18}O line at 1656 GHz (blue and red lines).

Observed and modeled spectra of the para- H_2^{18}O line at 1102 GHz and the ortho- H_2^{18}O line at 1656 GHz are shown in Figure 2. The H_2^{18}O (ortho+para) abundance in the envelope X_{out} , is 2.4×10^{-11} . The recommended isotopic abundance ratio between O^{16} and O^{18} is 500 (Lodders, 2003). Using this value, the H_2O abundance is 1.2×10^{-8} and the HDO/ H_2O abundance ratio is 5.8×10^{-3} in the outer envelope.

5 Summary

We derive HDO abundances of $X_{in} = (1.7\text{--}3.5) \times 10^{-8}$ (for $T \geq 100$ K) and $X_{out} = (7.0\text{--}10) \times 10^{-11}$ (for $T < 100$ K), (Table 7), in the three high-mass star forming regions. The inner HDO abundances are consistent with recent studies of high-mass protostars (Coutens et al., 2012; Fuente et al., 2012; Liu et al., 2013; Emprechtinger et al., 2013). We find somewhat different value of $X_{out}(\text{HDO})$ for G34.26 compared to Liu et al. (2013). This is probably because the 465 GHz line, which is very sensitive for X_{out} value is not well reproduced by their model.

Our model has a simple geometry and physical structure, it does not take radiative pumping or the turbulent velocity field, which is responsible for the line width, into account. Nevertheless the model is successful in reproducing the observed HDO integrated line intensities of the 465 GHz and 509 GHz transitions. These lines, especially the 465 GHz, ground-state transition, are the very good probes of the colder, outer regions. In the three hot cores we have studied, we find similar low values of the HDO/ H_2O abundance ratio.

Table 1: Source sample.

Source	α (J2000)	δ (J2000)	D (kpc)
G34.26+0.15	18 53 18.6	+01 14 57.7	3.7 ^a
W51e ₁ /e ₂	19 23 43.9	+14 30 25.9	5.4 ^b
W49N	19 10 13.2	+09 06 12.0	11.4 ^c

a Watt & Mundy (1999).

b Sato et al. (2010).

c Gwinn et al. (1992).

Table 2: Best fit model parameters.

Source	n_0 (cm^{-3})	T_0 (K)	X_{in} (HDO)	X_{out} (HDO)
W49N	4.0×10^8	250	2.0×10^{-8}	1.0×10^{-10}
W51e ₁ /e ₂	2.0×10^8	230	1.7×10^{-8}	0.7×10^{-10}
G34.26+0.15	1.0×10^8	200	3.5×10^{-8}	0.7×10^{-10}

References

- Beuther, H., Schilke, P., Menten, K. M., et al., *High-Mass Protostellar Candidates. II. Density Structure from Dust Continuum and CS Emission*, ApJ **566**, 945 (2002)
- Brown, P. D., Millar, T. J., *Models of the gas-grain interaction - Deuterium chemistry*, MNRAS **237**, 661 (1989)
- Campbell, M. F., Garland, C. A., Deutsh, L. K., et al., *Narrowband Mid-Infrared Images and Models of the H II Complex G34.3+0.2*, ApJ **536**, 816 (2000)
- Coutens, A., et al., *A study of deuterated water in the low-mass protostar IRAS 16293-2422*, A&A **539**, 132 (2012)
- Emprechtinger, M., et al., *The Abundance, Ortho/Para Ratio, and Deuteration of Water in the High-mass Star-forming Region NGC 6334 I*, ApJ **761**, 61 (2013)
- Fuente, A., Caselli, P., Coey, C. M., et al., *The abundance of C18O and HDO in the envelope and hot core of the intermediate mass protostar NGC 7129 FIRS 2*, A&A **540**, 75 (2012)
- Gwinn, C. R., Moran, J. M., M, R., *Models of the gas-grain interaction - Deuterium chemistry*, ApJ **393**, 149 (1992)
- Hatchell, J., van der Tak, F. F. S., *The physical structure of high-mass star-forming cores*, A&A **409**, 589 (2003)
- Hunter, T. R., Neugebauer, G., Benford, D. J., et al., *G34.24+0.13MM: A Deeply Embedded Proto-B-Star*, ApJ **493**, 97 (1998)
- Liu, F. C., Parise, B., Wyrowski, F., et al., *Water deuterium fractionation in the high-mass hot core G34.26+0.15*, A&A **550**, A37 (2013)
- Lodders, K., *Solar System Abundances and Condensation Temperatures of the Elements*, ApJ **591**, 1220L (2003)
- MacDonald, G. M., Gibb, A. G., Habing, R. J., Millar, T. J., *A 330-360 GHz spectral survey of G 34.3+0.15. I. Data and physical analysis.*, A&AS **119**, 333 (1996)
- Marseille, M. G., van der Tak, F. F. S., Herpin, F., Jacq, T., *Tracing early evolutionary stages of high-mass star formation with molecular lines*, A&A **522**, 74 (2010)
- Pety, J., *Successes of and Challenges to GILDAS, a State-of-the-Art Radioastronomy Toolkit*, in T. Casoli, J. M. Contini, L. Pagani (eds.) SF2A-2005: Semaine de l'Astrophysique Francaise, 721, Published by EdP-Sciences (2005)

- Reid, M. J., Ho, P. T. P., *G34.3 + 0.2 - A 'cometary' H II region*, ApJ **288**, L17 (1985)
- Sato, M., Reid, M. J., Brunthaler, A., Menten, K. M., *Trigonometric Parallax of W51 Main/South*, ApJ **720**, 1055 (2010)
- Shu, F. H., *Self-similar collapse of isothermal spheres and star formation*, ApJ **214**, 488 (1977)
- Tielens, A. G. G. M., *Surface chemistry of deuterated molecules*, A&A **119**, 177 (1983)
- Viti, S., Williams, D. A., *Time-dependent evaporation of icy mantles in hot cores*, MNRAS **305**, 755 (1999)
- Watt, S., Mundy, L. G., *Molecular Environments of Young Massive Stars: G34.26+0.15, G11.94-0.62, G33.92+0.11, and IRAS 18511+0146*, ApJS **125**, 143 (1999)
- Zmuidzinas, J., Blake, A., Carlstrom, J., et. al, *HCl Absorption Toward Sagittarius B2*, ApJ **447**, L125 (1995)